HHS Public Access

Author manuscript

Nat Cell Biol. Author manuscript; available in PMC 2017 October 10.

Published in final edited form as:

Nat Cell Biol. 2017 May ; 19(5): 457–467. doi:10.1038/ncb3508.

PDGF signaling guides neural crest contribution to the haematopoietic stem cell specification niche

Erich W. Damm and **Wilson K. Clements***

Department of Hematology, St. Jude Children's Research Hospital, 262 Danny Thomas Place, Memphis, TN, 38105, USA

Abstract

Haematopoietic stem cells (HSCs) support maintenance of the haematopoietic and immune systems throughout the life of vertebrates, and are the therapeutic component of bone marrow transplants. Understanding native specification of HSCs, to uncover key signals that might help improve *in vitro* directed differentiation protocols, has been a longstanding biomedical goal. The current impossibility of specifying true HSCs *in vitro* suggests that key signals remain unknown. We speculated that such signals might be presented by surrounding "niche" cells, but no such cells have been defined. Here we demonstrate in zebrafish, that trunk neural crest (NC) physically associate with HSC precursors in the dorsal aorta (DA) just prior to initiation of the definitive haematopoietic programme. Preventing association of the NC with the DA leads to loss of HSCs. Our results define NC as key cellular components of the HSC specification niche that can be profiled to identify unknown HSC specification signals.

Introduction

Haematopoeitic stem cells (HSCs) are the self-renewing population of cells that generate all the mature blood lineages throughout life and are the therapeutic component of bone marrow transplants[1]. There is considerable interest in directed differentiation of HSCs from iPSCs for transplant treatment of haematologic disorders; however, *in vitro* specification of normal HSCs with high level engraftment and normal multilineage potential has not yet been achieved, suggesting that key specification signals remain unknown. In all vertebrates, HSCs arise from haemogenic endothelium (HE) in the ventral floor of the dorsal (DA)[1–3]. Stromal cells residing in stem cell microenvironments often act as a "niche" to contribute important cues that regulate behavior[4]. HE cells likely receive specification signals from stromal cells constituting an HSC specification niche. To date, there have been no previous reports on the identity or origin of stromal cells required for HSC specification in the embryo, but such cells, if they exist, would be an important population to interrogate to find unknown

*Corresponding Author: Department of Hematology, St. Jude Children's Research Hospital, 262 Danny Thomas Place, Memphis, TN, 38105, USA, Phone: +1 901 595 5940, Fax: +1 901 595 4723, wilson.clements@stjude.org.

Author Contributions

E.W.D. and W.K.C. designed all experiments. E.W.D. performed all experiments. E.W.D. and W.K.C. analysed all results and wrote the manuscript.

specification signals. We hypothesized that cellular components of the specification niche might arise from migratory cells, providing a level of control over timing and presentation of inductive cues presented to the HE[1,5]. The zebrafish represents an ideal model vertebrate system in which to address the origin of niche cells, owing to the high level of conservation in programming of haematopoietic ontogeny[1] and its receptiveness to direct observation of cellular fate by time lapse confocal microscopy using transgenic fluorescence reporter lines.

Trunk neural crest (NC) are a migratory neural-ectoderm-derived cell population that contribute to diverse tissues in the embryo[6,7]. Trunk NC follow stereotypical migration routes, and give rise to a variety of adult structures including neurons, glia and endocrine cells of the parasympathetic and sympathetic nervous system (SNS), as well as pigment, depending on their location in the embryo[6,7,8]. An interplay of guidance cues and adhesive interactions controls migration and correct positioning of these cells[6,7,8]. Interestingly, trunk NC that become SNS neurons coalesce bilaterally along the length of the DA in zebrafish and mammals[8,9], positioning them within signaling range of HE cells.

Here we demonstrate that trunk NC physically associate with the DA just prior to initiation of the haematopoeitic programme and are in close proximity to nascent *runx1*$^{+}$ HSC precursors. We show that ventromedially directed migration of NC to the DA is dependent on Platelet derived growth factor (Pdgf) signaling, and that perturbing this path or other requirements for NC patterning leads to defective HSC specification. Interestingly, in mammals, trunk NC derivatives play important roles in the adult bone marrow HSC support niche[10,11]. Although the bone marrow niche is temporally, anatomically, and functionally distinct from the specification niche, NC contribution to both suggests a potential point of continuity. Our results define a previously unknown cellular component of the HSC specification niche in a vertebrate.

Results

Trunk NC contact the dorsal aorta prior to and during HSC specification

We wanted to identify the origin of cells in contact with HE of the DA immediately prior to initiation of the definitive haematopoietic programme. To investigate the possibility that NC might migrate to the DA at the right time and in sufficient proximity to regulate HSC specification, we carefully analysed their localization over the critical time window. We tracked NC positions over 11 hours of development, both by *in situ* hybridization for the zebrafish specific NC marker *crestin*[12] relative to the arterial marker *efnb2a* and by live time lapse confocal imaging in double transgenic (*Tg(fli1a:EGFP;sox10:mRFP)*) embryos where enhanced Green Fluorescent Protein (EGFP) is expressed in endothelial cells and membrane-bound Red Fluorescent Protein (mRFP) in NC (Fig. 1a–h, Supplementary Fig. 1 a–f, Supplementary Videos 1, 2). The ventral migration of trunk NC initiates rostrally in the embryo and proceeds caudally[6,7,12], with the first migration of cells that include SNS progenitors between somite and neural tube visible by 16 hours post fertilization (h.p.f.)[7,12] and continuing over the next several hours[12] with some streams reaching halfway around the notochord and others reaching the dorsal aspect of the DA by 20–21 h.p.f. (Fig. 1b–d, Supplementary Figs. 1a–b, Supplementary Videos 1, 2). By 23 h.p.f., the time when the onset of the definitive haematopoietic programme is first observable by expression of the

conserved HSC precursor marker *runx1* in the HE[1,3,5], trunk NC had migrated into close proximity with the DA (Fig. 1a–a′, f, i–i′, Supplementary Fig. 1 d, Supplementary Videos 1, 2). The second stream NC ventrolateral migration of pigment lineage precursors[7] between the overlying ectoderm and somite had also begun by this stage (Fig. 1i). By 24 h.p.f., NC were in contact with the DA endothelium in the sub-aortic space (Fig. 1g, j–j′, Supplementary Fig. 1 e). NC remained in close association with the vasculature through 30 h.p.f. and likely into adulthood, given their contribution to the SNS. Thus, trunk NC achieve close contact with the DA immediately prior to and during initiation of the definitive haematopoietic programme, and are therefore present at the right time and place to instruct HSC specification.

Pdgf signalling is required for ventromedial migration of trunk NC

If NC association with the DA is required for initiation of definitive haematopoietic programming, preventing this association should result in loss of HSCs. Pdgf signalling regulates key cell migration events in the embryo[13] including cranial NC migration[7,14], although the role of Pdgf signaling in trunk NC migration has not been well defined[14]. We confirmed expression of *pdgfra* and *pdgfrb* in trunk pre-migratory NC[15,16] (Supplementary Fig. 2 a–f″). Consistent with previous reports[16], we did not observe expression of either receptor in endothelial cells by *in situ* through 24 h.p.f., when HSC specification initiates (Supplementary Fig. 2 a–f″), excluding any cell-autonomous role for Pdgf signaling in HSC specification. We were, however, able to confirm the previously reported expression of *pdgfrb* in the floorplate and hypochord[16] as well as both receptors in the ventral somite[15,16]. Pdgfra interacts with Pdgfa (Pdgfaa and Pdgfab paralogues in zebrafish) and Pdgfc ligands, while Pdgfrb interacts with Pdgfb ligands[13]. We found that *pdgfab* and *pdgfc* are expressed in the medial aspect of the somite, along the ventromedial migratory route of trunk NC, prior to and during migration (E.W. Damm, in preparation). These results demonstrate that Pdgf receptors and ligands are expressed in a pattern consistent with a role in controlling migration of NC to axial structures like the DA.

We directly tested the requirement for Pdgf signaling in NC migration by examining trunk crest migratory behavior in embryos where Pdgf signaling was impaired by pharmacological inhibition, in animals where Pdgf receptors were knocked down by morpholino injection, and in animals mutant for Pdgfra (Fig. 2; Supplementary Fig. 3). Although the abundance of *crestin*$^{+}$ NC appeared unchanged in animals treated with the Pdgfr tyrosine kinase inhibitor V (inhV)[17], which inhibits both receptor isoforms, the progress of ventromedial trunk NC migration, was arrested at the horizontal myoseptum, approximately even with the notochord (Supplementary Fig. 3 a–b′, g). To confirm a requirement for Pdgf signaling we knocked down expression of individual receptors by injection of morpholinos targeting either *pdgfra*[18] or *pdgfrb*[16]. As with inhV treatment, *crestin* levels initially appeared normal, but NC migration was significantly arrested at the horizontal myoseptum (Fig. 2a–b′, e , Supplementary Fig. 3 c–e′, g). Interestingly, NC migration was only affected in 48% of Pdgfrb morphants (Supplementary Fig. 3 d–e′, g), whereas in Pdgfra single morphants and in Pdgfra/b double morphants, where PdgfraMO was injected at a sub-effective dose, migration defects were nearly fully penetrant and had not recovered by 36 h.p.f. (Supplementary Fig. 3 f–i). Since Pdgfra appeared to be the primary receptor required, we

confirmed this requirement in mutant animals carrying a hypomorphic allele of *pdgfra* (*pdgfra*^{b1059}; Ref. 19; Fig. 2c–e). Finally, we examined NC migration relative to axial vasculature by time lapse imaging in Pdgfra morphant *fli1a:EGFP;sox10:mRFP* double transgenic embryos (Fig. 2f–m; Supplementary Videos 1–4). Trunk NC delaminated normally from the neural tube and were migrating ventromedially between 20 h.p.f. and 21.5 h,.p.f. (Fig. 2h–j, Supplementary Fig. 4 a–c, Supplementary Videos 3, 4). At 23–24 h.p.f., when haematopoietic programming initiates, trunk NC in morphant animals had still not progressed beyond the limit of the ventral notochord (Fig. 2b, k, Supplementary Fig. 4 a–e, Supplementary Videos 3, 4), whereas they had contacted the DA in uninjected controls (Fig. 1, Supplementary Fig. 1 a–e, Supplementary Videos 1, 2). We never observed migration of NC streams beyond the ventral aspect of the notochord in Pdgfra morpholino-injected animals through 30 h.p.f. by time lapse (Supplementary Fig. 3 k, Supplementary Fig. 4, Supplementary Videos 3, 4), or 36 h.p.f. by *in situ* (Supplementary Fig. 3 h–i), and NC never contacted the DA (Fig. 2; Supplementary Fig. 1; Supplementary Fig. 3 h–k, Supplementary Videos 3, 4). Trunk NC migrating along the ventrolateral migration pathway, were unaffected (Supplementary Fig. 3 i, k). Our results demonstrate that Pdgf signalling is required for migration of medial stream trunk NC, likely SNS progenitors, beyond the ventral aspect of the notochord to a point of contact with the DA.

Pdgf signalling is required for HSC specification

Since NC association with the DA was prevented in Pdgfra deficient embryos, we examined specification of HSCs in these animals. We looked for expression of *runx1,* a master regulator and marker of definitive haematopoiesis[1,5,20] at 24 h.p.f. and *cmyb*$^{+}$ HSC precursors[20] at 33 h.p.f. in the DA. We also examined *rag1* expression in the paired thymi at 4 days post fertilization (d.p.f.), which labels T lymphocytes[1,21,22] that necessarily develop from an HSC precursor and are lost in embryos where definitive haematopoiesis fails[1,21,22]. HSCs and T cells were absent or dramatically reduced in Pdgfra inhibited embryos (Fig. 3a–n) demonstrating that Pdgfra-mediated signalling is required for the initiation of the haematopoietic programme and specification of HSCs. Double staining for *crestin* confirmed defective NC migration in HSC deficient animals (Figure 3a, d, g, j). The defect in T lymphocyte development was not due to a requirement for Pdgfr signaling in thymic immigration because inhibition of Pdgfr signaling with inhV only affected *rag1* expression if embryos were treated prior to the specification of HSCs (Supplementary Fig. 5 l–q) and not during developmental stages when thymic colonization is occurring. *Runx1*$^{+}$ cells were reduced or absent in the DA of inhV-treated embryos (Supplementary Figure 5 a, b, k) and in embryos conditionally expressing a heat shock inducible YFP-fused dominant negative *pdgfrb* transgene (*Tg(UAS:dnpdgfrb-YFP;hsp70l:GAL4)*; Supplementary Fig. 5 c–e, k)[16], which likely inhibits both Pdgfrs due to receptor heterodimerization[13]. HSC emergence from HE between 26 h.p.f. and 36 h.p.f.[3] can be visualized as GFP^{+}mCherry^{+} cells in *Tg(cmyb:GFP;kdrl:mCherry)* double transgenic embryos[3]. We observed a drastic reduction in the number of emerging HSCs in Pdgfra morphants compared to uninjected controls (Figure 3o–q). Last, we confirmed a recently published contribution of Pdgfrb signaling to HSC specification[23]. *Runx1*$^{+}$ cells were moderately reduced in about 41% of Pdgfrb morphants (Supplementary Fig. 5 f–h, k), phenocopying a *pdgfrb* mutant allele[23], and this reduction could be enhanced by co-injection of a sub-effective dose of Pdgfra morpholino

(Supplementary Fig. 5 f–k), indicating a genetic interaction between these receptors during initiation of the haematopoietic programme and that Pdgfra is the dominant receptor involved.

The presence of a normal DA is a pre-requisite for HSC specification[1,2,3], so we wanted to determine the integrity of pre-haematopoietic tissues in Pdgfr deficient embryos. The morphology of Pdgfra and Pdgfrb inhibited embryos was grossly normal at 24 – 26 h.p.f. (Supplementary Fig. 2 g–l), with beating hearts and circulating *gata1*$^{+}$ primitive erythroid cells (which do not derive from an HSC; Fig. 4a–c, s), although occasionally embryos exhibited yolk sac edema and a ventrally directed bend in the tail (Supplementary Fig. 2 g–l). Pre-haematopoietic mesoderm marked by *tal1* (also known as *scl*)[1,5] was present (Fig. 4d–f, s) and *cdh5* (also known as *ve-cadherin*) expression revealed normal endothelium[1,5] (Fig. 4g–i, s). Importantly, *efnb2a*, *notch1b* and *gata2b* expression together revealed that the DA and HE were present and patterned normally[1,5,24] (Fig. 4j–s). These results demonstrate that haematopoietic competent endothelium is present in Pdgfr signaling deficient embryos and suggest that the role of Pdgf signalling in HSC specification is to trigger initiation of the haematopoietic programme. As we did not observe Pdgf receptor expression in the endothelium itself (Supplementary Fig. 2 a–f″; and ref. 16) the requirement for Pdgf signaling must reflect its necessity in some other tissue such as NC, likely through regulation of availability of a relay signal.

Trunk NC association with the dorsal aorta is required for HSC specification

Our results are consistent with a model where trunk NC present a signal or signals to the HE that is required for HSC specification. NC make direct contact with nascent *runx1*$^{+}$ HSCs in the DA (Fig. 3r–r″) at high frequency (76%; n = 15 zebrafish embryos). These results suggest that NC interaction with HE is required for HSC specification; however, since *pdgfra* and *pdgfrb* are expressed in tissues beyond NC, we wanted to confirm that NC are indeed required by preventing crest specification or migration using multiple additional perturbations. *Transcription factor AP-2 alpha* (*Tfap2a*)[7,25], *sox10*[7,26] and *syndecan4* (*sdc4*)[7,27] are known regulators of NC specification and migration, and multiple morpholinos and mutants targeting these genes are available that allow independent means of disrupting NC association with the HE. None of these genes is expressed in the DA endothelium during HSC specification[25–27]. NC specification and migration was prevented and medial crest cells did not contact the DA in embryos injected with morpholinos targeting *tfap2a*, *sox10*, and *sdc4*, as well as in *tfap2a*^{ts213} and *sox10*^{m241} mutants (Fig. 5a, d, g, j, o; Supplementary Fig. 6 a, d, j, m, r; Supplementary Fig. 7 a–h)[25–27]. Interestingly, migration of ventromedially migrating NC that contact the DA was less strongly affected in the *sox10* mutant, *colorless*, despite severe defects in the development of the ventrolaterally migrating pigment precursors (Supplementary Fig. 6 g, j, r; Supplementary Fig. 7 e–f, x–x′). As previously described, the Sox10 morpholino phenocopied the pigment phenotype of the *sox10*^{m241} mutant[28] (Supplementary Fig. 7 v–v′), but had a stronger effect on the ventromedially migrating population of NC (Fig. 5a, d, o). The Tfap2aMO phenocopied the pigment development delay of the *tfap2a*^{ts213} mutant[25] (Supplementary Fig. 7 y–y′) and caused aberrant splicing of *tfap2a* mRNA (Supplementary Fig. 7 u) as described[25]. *Runx1*$^{+}$ and *cmyb*$^{+}$ cells in the DA at 24–26 h.p.f. and 33 h.p.f. respectively, as well as *rag1*$^{+}$ T

lymphocytes at 4 d.p.f were significantly reduced or absent in Tfap2a, Sox10 and Sdc4 morphant and in *tfap2a*^{ts213} and *sox10*^{m241} homozygous mutant embryos (Fig. 5a–n, Supplementary Figs. 6 a–q, 7 i–p), indicating defective HSC specification. Strikingly, rare *runx1*$^{+}$ cells that we were able to find in *sox10*^{m241} mutants, as well as Tfap2a and Sdc4 morphants that had only partial defects in ventromedial NC migration were usually at the locations where crest had reached the DA, strongly suggesting that close proximity is required for HSC specification (Supplementary Fig. 6 d, j, m). We further observed significantly reduced numbers of emerging HSCs at 36 h.p.f. in *Tg(cmyb:GFP;kdrl:mCherry)* embryos injected with Tfap2aMO, Sox10MO or Sdc4MO (Fig. 5p–s, Supplementary Fig. 6 s–u). Tfap2a, Sox10 and Sdc4 morphant embryos were grossly normal, had beating hearts and circulating primitive erythroid cells further confirmed by *gata1* expression (Fig. 6q–t, v–y′, Supplementary Fig. 7 a–d, y), although Sdc4 morphants occasionally exhibited a bend in the posterior aspect of the tail (Supplementary Fig. 7 s). The expression of *tal1, cdh5*, *efnb2a*, *notch1b*, and *gata2b* confirmed that as in Pdgfr deficient embryos, pre-haematopoietic tissues had developed normally in these animals (Fig. 6e–y). In all, ten independent means of preventing NC association with the pre-haematopoietic DA--pharmacologically, by five different morpholinos, one dominant negative transgenic, and three mutants--result in significantly impaired specification of HSCs. Our results demonstrate a requirement for the association of trunk NC with the DA for initiation of the haematopoietic programme and the specification of HSCs, likely by presentation of one or more short range inductive signals triggering the initiation of the haematopoietic programming.

Catecholamine neurotransmitters are not required for HSC specification

A previous report implicated SNS neurons, derivatives of early trunk NC, in the emergence of HSCs in mouse embryos through catecholamine neurotransmitter signalling[29]. Biosynthesis of catecholamines requires the enzymes *tyrosine hydroxylase* (*th*) and *dopamine-β-hydroxylase* (*dbh*)[8,30–32], both of which are also markers of overt SNS neuronal differentiation[31,32]. Expression of *th* and *dbh* in zebrafish trunk SNS neurons is not present until at least 36 h.p.f.[31], well after initiation of haematopoietic programming at 23–24 h.p.f. We confirmed that these genes were not expressed during the initiation of haematopoietic programming and that even by 5 d.p.f. expression was only present in the superior cervical ganglion (Fig. 7a–f). To confirm that early inductive signals are not catecholamine synthetic enzymes, we disrupted their synthesis with a morpholino against *th*[32]. Th morphants had normal numbers of *runx1* and *cmyb* expressing cells at 24 and 36 h.p.f. respectively, despite strongly reduced levels of *th* mRNA in morphants (Fig. 7g–m). Our results indicate that while catecholamine signalling may be important for early HSC maintenance, pre-neuronal trunk NC must contribute a different, earlier signal required for initiation of haematopoietic programming.

Discussion

Our results demonstrate that trunk NC migration to the DA, regulated by Pdgf signalling, is required for HSC specification. We propose that these cells contribute to a cellular HSC specification “niche”, although it is possible and likely that additional cell types may also be

required. NC likely present pro-haematopoietic inductive signals to haemogenic precursors in the HE and thus recommend themselves as a population to be interrogated to identify unknown HSC specification signals. The proximity of NC to *runx1*$^{+}$ cells, in wild-type embryos and in perturbations where there are rare, properly migrated NC suggests that such a signal is likely to act at short range.

Our results also provide a demonstration that Pdgf signalling regulates migration of the trunk NC. *Pdgfra* mutant mice and zebrafish exhibit severe craniofacial defects due to defective migration and increased apoptosis of the cranial NC[14,19,33], as well as aortic arch and ventricular septal defects as a result of defective cardiac NC migration[33]. In the trunk, we find that Pdgf signaling regulates specifically the ability of ventromedially migrating NC to pass the horizontal myoseptum, although whether the requirement is instructive or permissive is not clear. In all cases, *pdgfra* appears to be the key receptor involved[14,34,35]. NC in the trunk that follow the ventromedial migration path give rise notably to sympathetic neurons[7,8]. Pigment cell precursors, which migrate ventrolaterally, were unaffected. As sympathetic neurons remain in association with the DA to adulthood, it seems probable that NC-derived specification niche cells contribute to the SNS, although we cannot exclude the possibility that different derivatives are involved. Pdgf signalling also regulates migration of additional cell types, such as vascular smooth muscle cell precursors, so it is conceivable that the requirement for Pdgf signaling in establishing the specification niche extends beyond direction of NC.

NC contribute both to the specification niche and the adult homeostasis niche in the bone marrow; however the two regions are temporally, anatomically, and functionally distinct. Whereas the purpose of the specification niche is to establish the haematopoietic programme in endothelial cells *de novo* and promote the mobilization to embryonic expansion tissues while preserving stemness, the adult niche directs diverse behaviors, such as choices between quiescence and proliferation, self-renewal and differentiation, circadian egress, and probably lineage priming[36,37]. The bone marrow contains at least two kinds of trunk NC derivatives: sympathetic neurons and nestin^{+} mesenchymal stem cells (MSCs)[10,11,36–38]. Nestin^{+} MSCs are perivascular cells that regulate HSC quiescence and are innervated by adrenergic sympathetic neurons[36–39]. At least some of these MSCs are PDGFRα^{+} and have HSC support activity[40]. Sympathetic neurons regulate mobilization of HSCs from the adult niche by stimulating noradrenergic signaling-dependent downregulation of CXCL12 (also known as SDF1)[11,38]. Thus NC or their derivatives direct stem and mobilization behaviors both during HSC specification and in the adult niche, raising the possibility that the same or similar HSC signal transduction programmes are activated in both cases. As we move forward, it will be important to better understand the molecular nature of the NC embryonic HSC specification signals, both for use in directed differentiation and possibly as a tool for regulation of adult HSCs.

Methods

Zebrafish husbandry

Zebrafish *WIK*, *Tg(hsp70l:GAL4; UAS:dnpdgfrb)*$^{kca4;\ sr1}$, *Tg(−7.2sox10:mRFP)*^{vu234}, *Tg(fli1a:EGFP)*^{y1}, *Tg(cmyb:GFP; kdrl-mCherry)*, *tfap2a*^{ts213}, *sox10*^{m241} and *pdgfra*^{b1059}

animals were maintained, raised, crossed, staged and injected as previously described[41], under an approved IACUC protocol, and in compliance with all IACUC and AVMA guidelines. Embryos were not preferentially selected by sex.

Morpholinos, injections and heat shock

Morpholino oligonucleotides (Gene Tools) targeting *pdgfra*, *pdgfrb*, *sox10*, *tfap2a*, *sdc4* and *th* were injected as described[41] into one-cell embryos. See Supplementary Table 1 for morpholino sequences and concentrations. For heat shock experiments, *Tg(UAS:dnpdgfrb-YFP;hsp70:GAL4)*[16] fish were crossed to *Tg(hsp70:GAL4)* fish and progeny were heat shocked at 40° C for 30 minutes[16]. YFP+ and YFP- heat shocked and non-heat shocked sibling embryos were sorted at 16 h.p.f. for subsequent experiments.

Cloning, constructs, probes and RT-PCR

Pdgfra (RefSeq: NM_131459) was amplified from 24 h.p.f. cDNA, *th* (RefSeq: NM_131149) and *dbh* (RefSeq: NM_001109694) were amplified from 96 h.p.f. cDNA. *WIK* strain cDNA was used in all cases. See Supplementary Table 1 for primer sequences. PCR reactions were run with an annealing temperature of 52° C for 35 cycles. *Pdgfra* was cloned into pCS2+, *th* and *dbh* were cloned into pCRII-TOPO (Invitrogen). *In situ* hybridization probes were produced as previously described[42] using either digoxigenin or fluorescein labeled NTPs (Roche), constructs were linearized (restriction enzymes from NEB) and transcribed (polymerase from Roche) with: pCS2+ *runx1* (EcoRI, T7; C. Burns), pBK-CMV *cmyb* (BamHI,T7; L. Zon), pCRII *rag1* (HindIII, T7; N. Trede), pBS *efnb2a* (XhoI, T3)[4], pBK-CMV *tal1* (SalI, T7; L. Zon), pBS *gata1* (Xba1, T7; D. Ransom), pExpress-1 *gata2b* (NheI, T7; D. Traver), pCRII *crestin* (BamHI, T7)[4], pCR-Script *notch1b* (BamHI, T3; M. Lardelli), pJC53.2 *pdgfrb* (XmaI, SP6; B. Appel), pCS2+ *pdgfra* (NotI, SP6), pCRII-TOPO *th* (XbaI, SP6), pCRII-TOPO *dbh* (NotI, SP6). For RT-PCR experiments, RNA was isolated from uninjected, Th morphant or Tfap2a morphant 24 h.p.f. embryos using Trizol Reagent (Ambion) according to the manufacturer's instructions and purified by phenol:chloroform:isoamyl alcohol extraction. cDNA was generated from purified RNA using the SuperScript III First-Strand Synthesis System for RT-PCR (Invitrogen) according to the manufacturer's instructions. PCR reactions were run with an annealing temperature of 51 degrees Celsius for 34 cycles and products were visualized on a 1% agarose gel. Product sizes were determined by comparing product bands with bands of known size from the GeneRuler DNA Ladder Mix (Invitrogen #SM0331).

Whole-mount *in situ* hybridization (WISH), microscopy and embryo sectioning

Whole mount *in situ* hybridization was performed as previously described[42]. NBT/BCIP solution (Roche) and Fast Red solution (Sigma) were used for the colorimetric reaction to detect digoxigenin and fluorescein labelled probes respectively. For all embryos where *in situ* hybridization was to be performed after 22 h.p.f., except *tfap2a* and *sox10* mutants and where *th* or *dbh* expression was to be examined, melanin production was inhibited by treatment of embryos with 1-Phenyl-2-thiourea (PTU) at 22 h.p.f. Since the development of pigment in *tfap2a* and *sox10* mutants was used as an indicator of the zygosity of the mutant alleles, pigmentation was either left intact or embryos were bleached post-fixation by hydrogen peroxide treatment[42]. For embryos being examined for *th* and *dbh* expression,

hydrogen peroxide treatment[42] was used to remove pigment as PTU treatment has been shown to inhibit the development of catecholaminergic neurons[43]. Embryos were photographed in 3% methyl cellulose using a Leica DFC310FX camera mounted on a Leica M205FA stereoscope. Unless otherwise indicated, at least three independent clutches of embryos were examined in each experiment. For quantification of *runx1* and *cmyb* expressing cells, unless otherwise indicated, 20 embryos from three independent clutches were quantified. In all cases except for experiments involving the *pdgfra*^{b1059} allele, the quantified embryos were randomly selected. For experiments involving the *pdgfra*^{b1059} allele, homozygous embryos were inferred based on phenotypic ratio and phenocopy of the Pdgfra morphant phenotype. Confocal images of live embryos and fixed tissues were acquired using a Nikon C2 laser scanning confocal system using a 20X Plan-Apo (0.75 NA) or a 40X Plan-Fluor (1.3 NA) lens as indicated. For live z-stack time lapse imaging, embryos were anesthetized in 0.04% tricaine solution and embedded in 0.4% low melting point agarose, z-stack thickness ranged from 40 μm to 50 μm with an optical section thickness ranging from 2 μm to 2.5 μm, time lapse length was 10 hours, pinhole size: 1.2 AU, with 488nm and 561nm laser lines set at 5% power. Five uninjected and five PdgfraMO injected embryos were filmed in total, each was from a different clutch and filmed on different days. Analysis was performed with Nikon Elements 4.30. *Tg(cmyb:GFP; kdrl:mCherry)* embryos were fixed with 4% paraformaldehyde at the stages indicated and were embedded in 4% low melt agarose prior to imaging. Confocal Z-stacks of *Tg(cmyb:GFP; kdrl:mCherry*) embryos ranged between 30 μm and 40 μm with an optical section thickness of 2.5 μm and the 488 nm and 561 nm laser lines set at 10% and 5% respectively, pinhole size: 1.2 AU. *Tg(fli1a:EGFP; sox10:mRFP)* embryos were fixed in 4% paraformaldehyde and embedded in 3.5% agarose. 50 μm sections were generated on a Leica VT1200 vibratome and mounted in glass bottom dishes (MatTek) for imaging on the confocal microscope, pinhole size: 1.2 AU, 488 nm laser power: 10%, 561 nm laser power: 5%.

Genotyping

Sox10^{m241} or *tfap2a*^{ts213} homozygous embryos were identified by established defects in embryo pigmentation and additionally, defective neural crest cell migration as indicated by *crestin* expression[26,27]. For *pdgfra*^{b1059} embryos, numbers of embryos indicate the fraction of total embryos in a heterozygous-incross-derived clutch—which included wild type, heterozygous, and homozygous individuals—that display the depicted phenotype. Genotype conclusions were inferred from NC migratory and hematopoietic phenotype. Observed phenotypic percentages, 21/99 embryos (21.2%) scored as decreased *runx1*, 18/85 (21.2%) decreased *cmyb*, and 19/72 (26.3%) decreased *rag1*, roughly conform to the expectation of 25% homozygous mutant individuals from a heterozygous incross. NC migration phenotypes, in embryos old enough, cosegregate with and confirm genotypic assignment.

Statistics and Reproducibility

The student's t-test was used with a 95% confidence level for all experiments. Unless otherwise indicated, at least three independent clutches of embryos were examined. No statistical method was used to predetermine sample size. Individual embryos were selected from pools of embryos and assigned to uninjected or morpholino injected categories randomly. Individual uninjected, morphant, wild type and mutant embryos were randomly

selected for examination of gene expression and time lapse microscopy. The investigators were not blinded to allocation during experiments and outcome assessment. Total embryo numbers are indicated in the figure legends or Supplementary Table 2.

Data Availability

Source data supporting Fig. 2 e, 3 m–o, 5 m–o, s, 6 y, 7 l, m and Supplementary Fig. 3 g, 5 k, 6 p–r, u have been provided as Supplementary Table 3. All other data supporting the findings of this study are available from the corresponding author upon reasonable request.

Supplementary Material

Refer to Web version on PubMed Central for supplementary material.

Acknowledgments

The authors thank B. Appel, C. Burns, M. Lardelli, D. Ransom, D. Traver, N. Trede and L. Zon for probe constructs; J. Eberhart, M. Granato, C. Lien, R. Stewart and D. Traver for providing mutant and transgenic zebrafish lines. We would also like to thank Jennifer Peters and Vickie Frohlich of the St. Jude Cell and Tissue Imaging Center for assistance with microscopy and Mitch Weiss for providing critical feedback on the manuscript. This work was funded by NIH R00HL097150 and March of Dimes Basil O'Connor Starter Scholar Research Award #5-FY14-42 to W.K.C.

References

1. Clements WK, Traver D. Signalling pathways that control vertebrate haematopoietic stem cell specification. Nat Rev Immunol. 2013; 13:336–348. [PubMed: 23618830]
2. Boisset JC, et al. In vivo imaging of haematopoietic cells emerging from the mouse aortic endothelium. Nature. 2010; 464:116–120. [PubMed: 20154729]
3. Bertrand JY, et al. Haematopoietic stem cells derive directly from aortic endothelium during development. Nature. 2010; 464:108–111. [PubMed: 20154733]
4. Scadden DT. Nice neighborhood: emerging concepts of the stem cell niche. Cell. 2014; 157:41–50. [PubMed: 24679525]
5. Clements WK, et al. A somitic Wnt16/Notch pathway specifies haematopoietic stem cells. Nature. 2011; 474:220–224. [PubMed: 21654806]
6. Shellard A, Mayor R. Chemotaxis during neural crest migration. Semin Cell Dev Biol. 2016; doi: 10.1016/j.semcdb.2016.01.031
7. Theveneau E, Mayor R. Neural crest delamination and migration: from epithelium-to-mesenchyme transition to collective cell migration. Developmental Biology. 2012; 366:34–54. [PubMed: 22261150]
8. Stewart RA, et al. Studying peripheral sympathetic nervous system development and neuroblastoma in zebrafish. Methods Cell Biol. 2010; 100:127–152. [PubMed: 21111216]
9. Serbedzija GN, Fraser SE, Bronner-Fraser M. Pathways of trunk neural crest cell migration in the mouse embryo as revealed by vital dye labelling. Development. 1990; 108:605–612. [PubMed: 2387238]
10. Isern J, et al. The neural crest is a source of mesenchymal stem cells with specialized hematopoietic stem cell niche function. Elife. 2014; 3:e03696. [PubMed: 25255216]
11. Katayama Y, et al. Signals from the sympathetic nervous system regulate hematopoietic stem cell egress from bone marrow. Cell. 2006; 124:407–421. [PubMed: 16439213]
12. Luo R, An M, Arduini BL, Henion PD. Specific pan-neural crest expression of zebrafish Crestin throughout embryonic development. Dev Dyn. 2001; 220:169–174. [PubMed: 11169850]
13. Andrae J, Gallini R, Betsholtz C. Role of platelet-derived growth factors in physiology and medicine. Genes Dev. 2008; 22:1276–1312. [PubMed: 18483217]

14. Smith CL, Tallquist MD. PDGF function in diverse neural crest cell populations. Cell Adh Migr. 2010; 4:561–566. [PubMed: 20657170]
15. Liu L, Chong SW, Balasubramaniyan NV, Korzh V, Ge R. Platelet-derived growth factor receptor alpha (pdgfr-alpha) gene in zebrafish embryonic development. Mech Dev. 2002; 116:227–230. [PubMed: 12128230]
16. Wiens KM, et al. Platelet-derived growth factor receptor beta is critical for zebrafish intersegmental vessel formation. PLoS ONE. 2010; 5:e11324. [PubMed: 20593033]
17. Nishioka C, et al. Ki11502, a novel multitargeted receptor tyrosine kinase inhibitor, induces growth arrest and apoptosis of human leukemia cells in vitro and in vivo. Blood. 2008; 111:5086–5092. [PubMed: 18309036]
18. Kartopawiro J, et al. Arap3 is dysregulated in a mouse model of hypotrichosis-lymphedema-telangiectasia and regulates lymphatic vascular development. Human Molecular Genetics. 2014; 23:1286–1297. [PubMed: 24163130]
19. Eberhart JK, et al. MicroRNA Mirn140 modulates Pdgf signaling during palatogenesis. Nat Genet. 2008; 40:290–298. [PubMed: 18264099]
20. Gering M, Patient R. Notch signalling and haematopoietic stem cell formation during embryogenesis. J Cell Physiol. 2010; 222:11–16. [PubMed: 19725072]
21. Kissa K, et al. Live imaging of emerging hematopoietic stem cells and early thymus colonization. Blood. 2008; 111:1147–1156. [PubMed: 17934068]
22. Yokota T, et al. Tracing the first waves of lymphopoiesis in mice. Development. 2006; 133:2041–2051. [PubMed: 16611687]
23. Lim S, et al. HIF1α-induced PDGFRβ signaling promotes developmental HSC production via IL-6 activation. Experimental Hematology. 2016; doi: 10.1016/j.exphem.201610002
24. Kim AD, et al. Discrete Notch signaling requirements in the specification of hematopoietic stem cells. EMBO J. 2014; doi: 10.15252/embj.201488784
25. Knight RD, et al. lockjaw encodes a zebrafish tfap2a required for early neural crest development. Development. 2003; 130:5755–5768. [PubMed: 14534133]
26. Dutton KA, et al. Zebrafish *colourless* encodes *sox10* and specifies non-ectomesenchymal neural crest fates. Development. 2001a; 128:4113–4125. [PubMed: 11684650]
27. Matthews HK, et al. Directional migration of neural crest cells in vivo is regulated by Syndecan-4/Rac1 and non-canonical Wnt signaling/RhoA. Development. 2008; 135:1771–1780. [PubMed: 18403410]
28. Dutton KA. A morpholino phenocopy of the *colourless* mutant. Genesis. 2001b; 30:188–0189. [PubMed: 11477705]
29. Fitch SR, et al. Signaling from the Sympathetic Nervous System Regulates Hematopoietic Stem Cell Emergence during Embryogenesis. Stem Cell. 2012; 11:554–566.
30. Huber K. The sympathoadrenal cell lineage: specification, diversification, and new perspectives. Developmental Biology. 2006; 298:335–343. [PubMed: 16928368]
31. An M, Luo R, Henion PD. Differentiation and maturation of zebrafish dorsal root and sympathetic ganglion neurons. J Comp Neurol. 2002; 446:267–275. [PubMed: 11932942]
32. Formella I, et al. Transient knockdown of tyrosine hydroxylase during development has persistent effects on behavior in adult zebrafish (*Danio rerio*). PLoS ONE. 2012; 7(8):e42482.doi: 10.1371/journal.pone.0042482 [PubMed: 22879998]
33. Tallquist MD, et al. Cell autonomous requirement for PDGFRalpha in populations of cranial and cardiac neural crest cells. Development. 2003; 130:507–518. [PubMed: 12490557]
34. Richarte AM, et al. Cooperation between the PDGF receptors in cardiac neural crest cell migration. Dev Biol. 2007; 306:785–796. [PubMed: 17499702]
35. McCarthy N, et al. Pdgfra and Pdgfrb genetically interact during craniofacial development. Dev Dyn. 2016; 245(6):641–652. [PubMed: 26971580]
36. Boulais PE, et al. Making sense of hematopoietic stem cell niches. Blood. 2015; 125(17):2621–2629. [PubMed: 25762174]
37. Morrison SJ, et al. The bone marrow niche for haematopoietic stem cells. Nature. 2014; 505:327–334. [PubMed: 24429631]

38. Mendez-Ferrer S, et al. Mesenchymal and hematopoietic stem cells form a unique bone marrow niche. Nature. 2010; 466:829–834. [PubMed: 20703299]

39. Kunisaki Y, et al. Arteriolar niches maintain haematopoietic stem cell quiescence. Nature. 2013; 502:637–643. [PubMed: 24107994]

40. Pinho S, et al. PDGFRα and CD51 mark human nestin^{+} sphere-forming mesenchymal stem cells capable of hematopoietic progenitor cell expansion. J Exp Med. 2013; 210(7):1351–1367. [PubMed: 23776077]

41. Westerfield, M. A Guide for the Laboratory Use of Zebrafish (Danio rerio). Univ. Oregon Press; 2004. The Zebrafish Book.

42. Thisse C, Thisse B. High-resolution *in situ* hybridization to whole-mount zebrafish embryos. Nat Protocols. 2008; 3:59–69. [PubMed: 18193022]

43. Higashi Y, et al. Inhibition of tyrosinase reduces cell viability in catecholaminergic neuronal cells. J Neurochem. 2000; 75:1771–1774. [PubMed: 10987861]

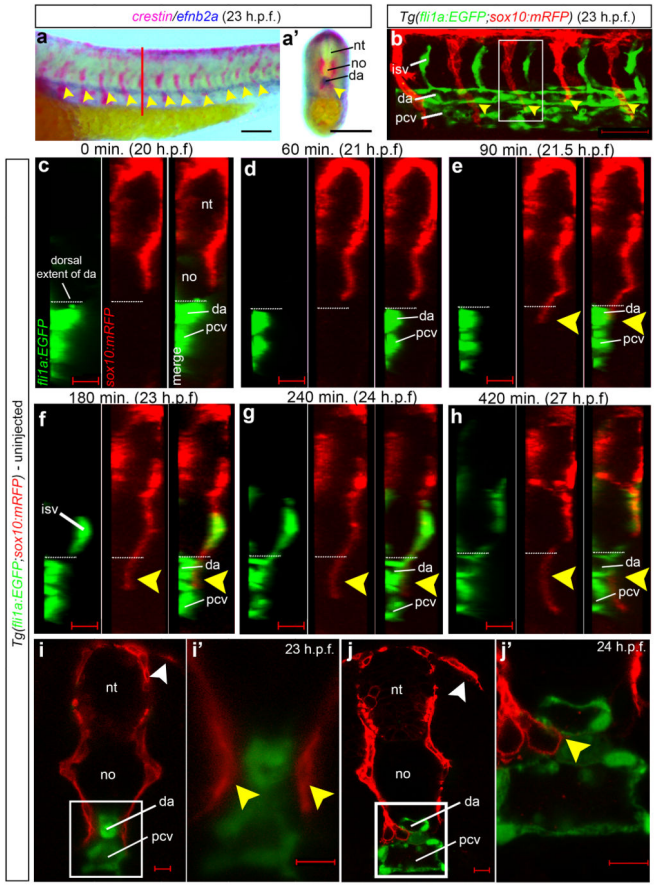

Figure 1. NC contact the DA prior to and during HSC specification

Progress of NC migration, marked by *crestin* expression relative to the DA, marked by *efnb2a* expression in trunk lateral view (**a**; dorsal up, anterior left) or in transverse section of the same embryo (**a′**; dorsal up) at 23 h.p.f. Level of transverse section is indicated (red bar, **a**), yellow arrowheads indicate ventral limit of NC progress (**a–b**). Scale bars = 100 μm. Live lateral z-stack volume projection of NC migration through the trunk using the NC reporter *sox10:mRFP* in comparison to *fli1a:EGFP* labelled endothelium, scale bar = 100 μm (**b**) or still images of virtual transverse trunk sections from the same embryo with dorsal up in single and merged channels (**c–h**) from time lapse confocal microscopy from 20 h.p.f. to 27 h.p.f. Dorsal extent of the DA is indicated by the dotted line, position of the transverse section projection is indicated by the white box in (**b**), scale bar = 50 μm, mag. = 200X. Confocal transverse mid-trunk section (dorsal up) at 23 h.p.f. (**i–i′**) and 24 h.p.f. (**j–j′**) showing proximity of NC to the DA, mag. = 400X, scale bar = 50 μm (**i, j**). White boxes in (**i–j**) indicates zoomed region in (**i′–j′**), yellow arrowheads in (**i′–j′**) indicate NC in close proximity to the DA, white arrowheads indicate cells of the pigment cell lineage migrating ventrolaterally (**i, j**), scale bar = 50 μm (**i′, j′**). nt – neural tube, no – notochord, da – dorsal aorta, pcv – posterior cardinal vein, isv – intersegmental vessel.

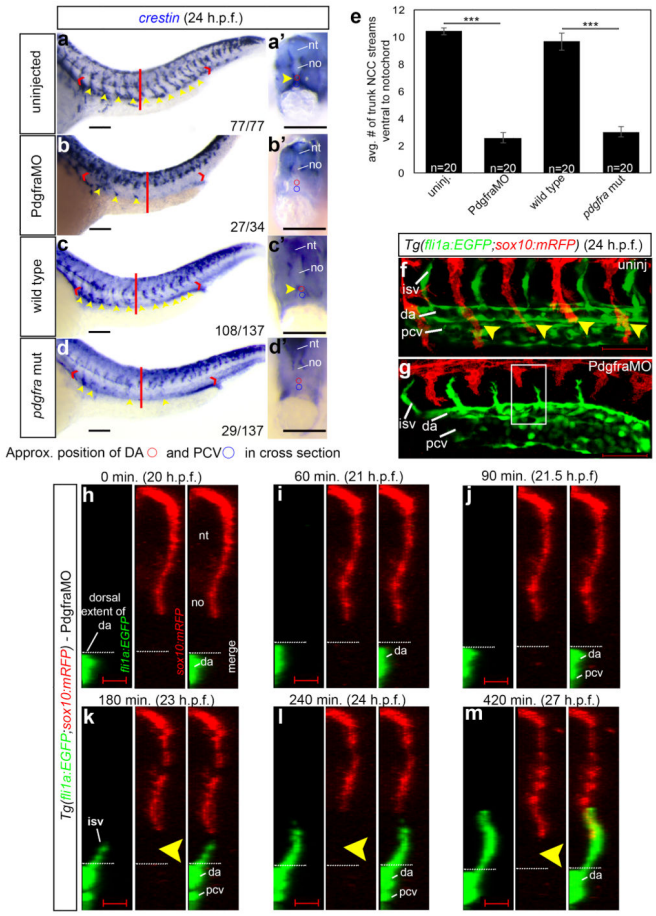

Figure 2. Pdgfra-mediated signalling is required for NC migration to the DA

Progress of NC migration marked by *crestin* expression in trunk lateral view (**a–d**; dorsal up, anterior left) or transverse section (dorsal up; **a′–d′**; DA, red circle; PCV, blue circle) in uninjected (**a, a′**), Pdgfra morphant (**b, b′**), wild-type and *pdgfra*^{b1059} heterozygotes (**c, c′**), and in *pdgfra*^{b1059} homozygous mutant sibling (**d, d′**) embryos, revealing the extent of NC migration at 24 h.p.f., transverse section position is indicated by red bars in (**a–d**), NC streams that have migrated ventral to the notochord are indicated by yellow arrowheads, red brackets enclose the DA-NC interaction region. Numbers in the bottom right corner of panels indicate numbers of zebrafish embryos analysed for the indicated gene, versus the total number of zebrafish analysed. Zebrafish randomly selected from three clutches are represented by the image (**a–d′**). Scale bars = 100 μm. *Pdgfra*^{b1059} homozygotes were inferred based on phenotypic ratio and phenocopy of the Pdgfra morphant NC and haematopoietic phenotypes. Average number of NC streams that have migrated ventral to the notochord for each condition (n = 20 zebrafish embryos each, randomly selected from three clutches each), triple asterisk indicates p-values < 0.0001 by student's T-test for each, error bars indicate standard error of the mean (**e**). See Supplementary Table 3. Lateral z-stack volume projections of the trunk (dorsal up, anterior left) with NC in red (*sox10:mRFP*) and vasculature in green (*fli1a:EGFP*) of an uninjected embryo (**f**) and a Pdgfra morphant embryo (**g**), scale bar = 100 μm, and still images of virtual transverse trunk sections with dorsal up in single and merged channels from time lapse confocal microscopy from 20 h.p.f.

to 27 h.p.f. as indicated (**h–m**), level of the section is indicated by the white box in (**g**), ventral progress of NC migration is indicated by yellow arrowheads (**f**, **k–m**), dotted line indicates the dorsal extent of the DA (**h–m**) scale bars = 50 μm. nt – neural tube, no – notochord, da – dorsal aorta, pcv – posterior cardinal vein, isv – intersegmental vessel.

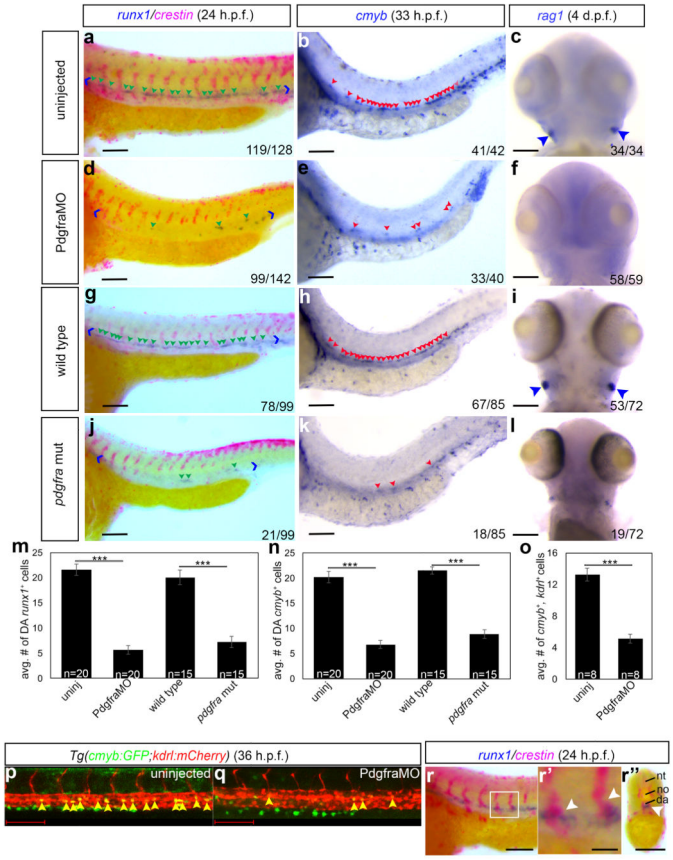

Figure 3. Pdgfra is required for HSC specification

Lateral trunk views (dorsal up, anterior left) of expression of the HSC marker *runx1* (blue) and the NC marker *crestin* (red; **a, d, g, j**), the HSC marker *cmyb* (**b, e, h, k**), and ventral head views of the T lymphocyte marker *rag1* (**c, f, i, l**) in uninjected (**a–c**), Pdgfra morphant (**d–f**), wild-type and *pdgfra*^{b1059} heterozygous (**g–i**), and *pdgfra*^{b1059} homozygous mutant sibling (**j–l**) embryos at the times indicated. Green arrowheads *runx1*$^{+}$, red arrowheads *cmyb*$^{+}$, blue arrowheads *rag1*$^{+}$ cells when present (**a–l**), blue brackets enclose the DA-NC interaction region (**a, d, g, j**). Numbers in bottom right corner indicate numbers of zebrafish embryos analysed for the indicated gene, versus the total number of zebrafish analysed. Zebrafish randomly selected from three clutches are represented by the image (**a–l**). Scale bars = 100 μm. Average number of *runx1*$^{+}$ (**m**) or *cmyb*$^{+}$ (**n**) cells in each condition (for uninjected and Pdgfra morphants, 20 zebrafish embryos were randomly selected from three clutches; for wild type and *pdgfra* mutants, 20 zebrafish embryos exhibiting the phenotypes (inferred mutants) displayed in (**g–l**) were selected from three clutches). Average number of mCherry^{+}GFP^{+} cells in the DA in each condition (**o**) (n = 8 zebrafish embryos from two clutches each). Error bars indicate standard error of the mean (**m–o**). Triple asterisk indicates p-values < 0.0001 by student's T-test for each (**m–o**). See Supplementary Table 3. Close up lateral views of the trunk vasculature with fluorescently labelled HSCs in uninjected (**p**) and Pdgfra morphant (**q**) *cmyb:GFP;kdrl:mCherry* transgenic embryos at 36 h.p.f., HSCs are yellow cells indicated by yellow arrowheads. Scale bar = 50 μm, mag. = 200X. Colocalization (indicated by white arrowheads) of *runx1*$^{+}$ (blue) in a lateral trunk

view of the DA and *crestin*$^{+}$ NC (red), scale bar = 100 μm and 50 μm respectively. (**r, r′**) and cross-section, scale bar = 100 μm. (**r″**) at 24 h.p.f. Mag. = 160X. nt – neural tube, no – notochord, da – dorsal aorta.

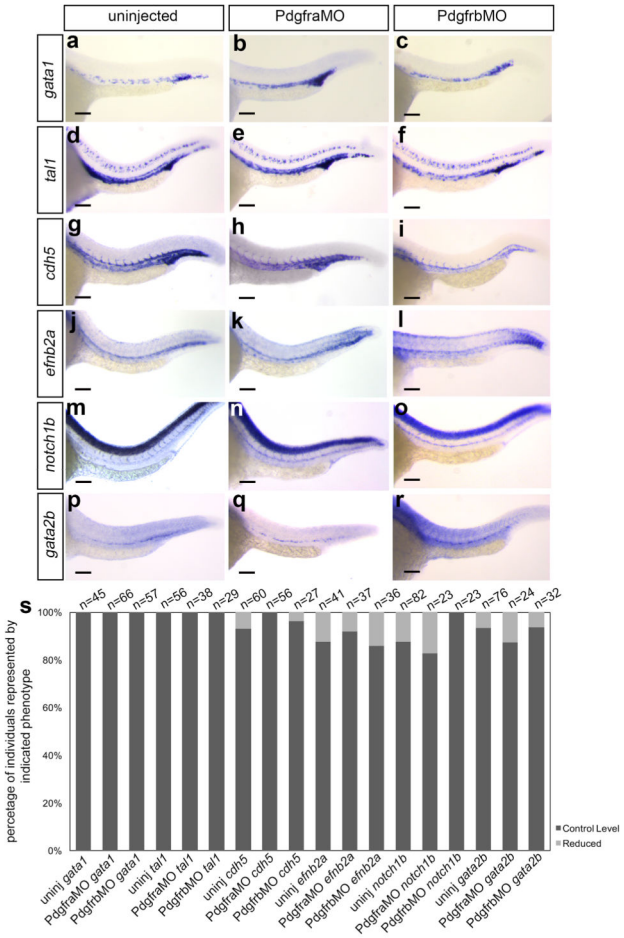

Figure 4. Arterial HE and primitive blood are normal in Pdgfra and Pdgfrb impaired animals

Lateral trunk views (dorsal up, anterior left) of *in situs* for markers for primitive erythrocytes (*gata1*, **a–c**) pre-haematopoietic mesoderm (*tal1*, **d–f**) vascular endothelium (*cdh5*, **g–i**), arterial identity (*efnb2a*, **j–l**; *notch1b*, **m–o**) and haemogenic endothelium (*gata2b*, **p–r**) in uninjected (left column), PdgfraMO (central column) and PdgfrbMO (right column) embryos at 24 h.p.f. Scale bars = 100 μm. Percentages of embryos exhibiting the specified phenotypes relative to the appearance of expression in uninjected controls with total number (n) of embryos examined (**s**). See Supplementary Table 2.

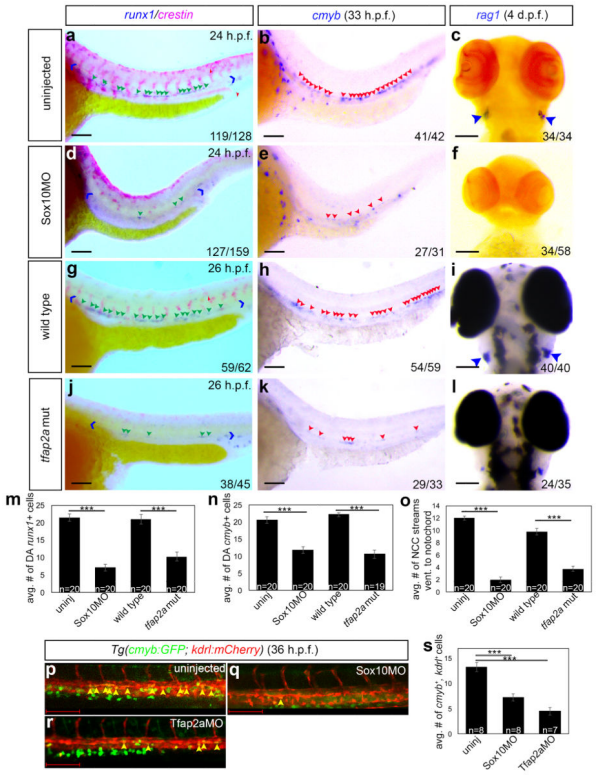

Figure 5. NC are required for HSCs

Lateral trunk views (dorsal up, anterior left) of expression of the HSC marker *runx1* (blue) and the NC marker *crestin* (red; **a, d, g, j**), the HSC marker *cmyb* (**b, e, h, k**) and ventral head views of the T lymphocyte marker *rag1* (**c, f, i, l**) in uninjected (**a–c**), Sox10 morphant (**d–f**), wild-type and *tfap2a*^{ts213} heterozygous (**g–i**), and *tfap2a*^{ts213} homozygous mutant (**j–l**) embryos at the times indicated. Green arrowheads *runx1*$^{+}$, red arrowheads *cmyb*$^{+}$, blue arrowheads *rag1*$^{+}$ cells when present, blue brackets enclose the DA-NC interaction region (**a, d, g, j**). Numbers in the bottom right corner of panels indicate numbers of zebrafish embryos analysed for the indicated gene, versus the total number of zebrafish analysed. Zebrafish randomly selected from three clutches are represented by the image (**a–l**). Scale bars = 100 μm. Average number of *runx1*$^{+}$ (**m**) or *cmyb*$^{+}$ (**n**) cells in each condition and average number of NC streams ventral to the notochord at 24 h.p.f. for the indicated conditions (**o**) (n=20 randomly selected zebrafish embryos from three clutches each; **m–o).** Close up lateral views of the trunk vasculature with fluorescently labelled HSCs in uninjected (**p**) Sox10 morphant (**q**) and Tfap2a morphant (**r**) *cmyb:GFP;kdrl:mCherry* transgenic embryos at 36 h.p.f., HSCs are yellow cells indicated by yellow arrowheads, scale bar = 50 μm, mag. = 200X. Average number of mCherry^{+}GFP^{+} cells in the DA in each condition (**s**) n = 8 zebrafish embryos (**p–q**), and n=7 zebrafish embryos for (**r**) from two clutches. Error bars indicate the standard error of the mean (**m–o, s**). Triple asterisk indicates p-values < 0.0001 by student's T-test for (**m–o**), p = 0.0004 for (**s**). See Supplementary Table 3.

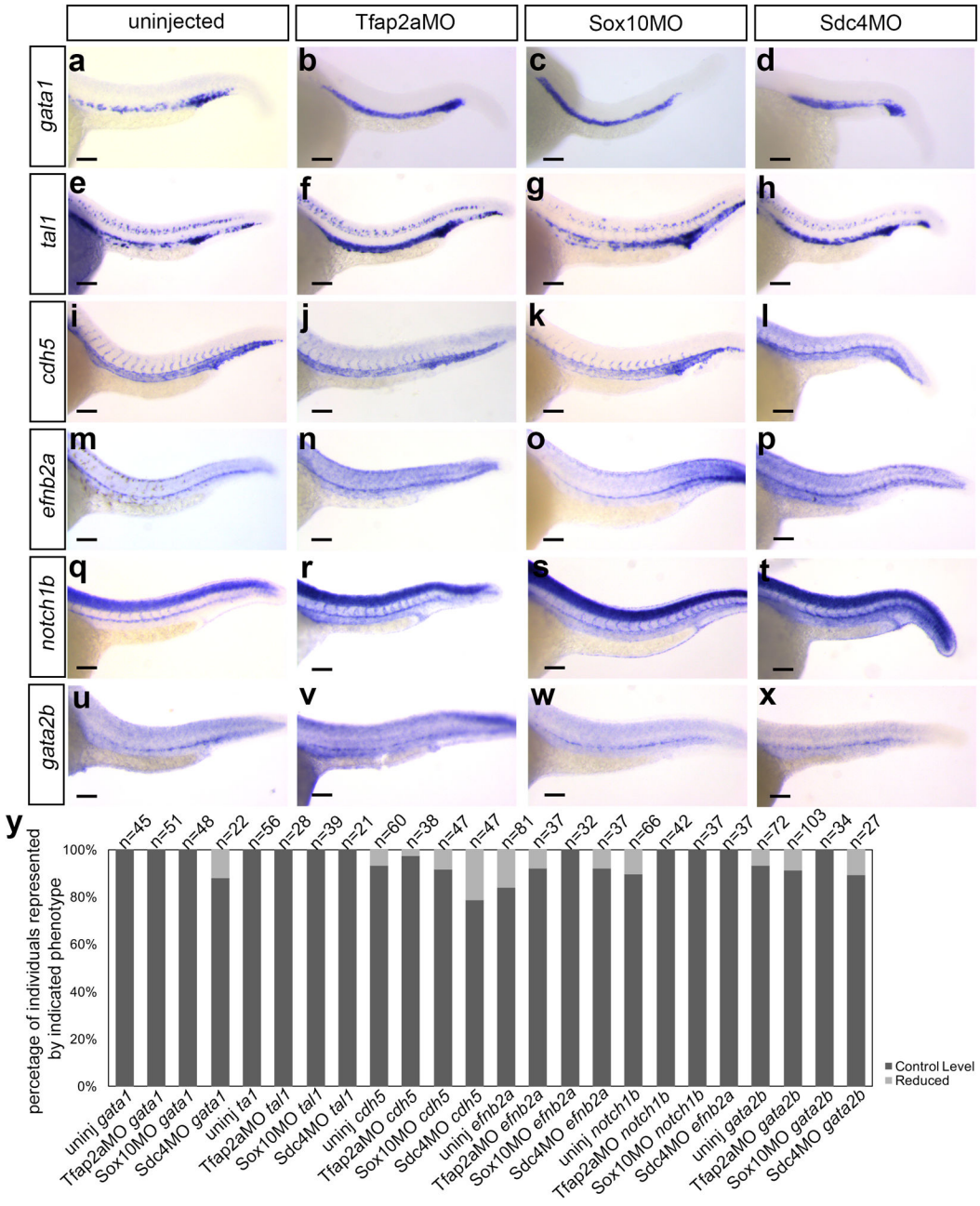

Figure 6. Arterial HE and primitive blood are normal in NC impaired animals

Lateral trunk views (dorsal up, anterior left) of *in situs* for markers of primitive erythrocytes (*gata1*, **a–d**), pre-haematopoietic mesoderm (*tal1*, **e–h**), vascular endothelium (*cdh5*, **i–l**), arterial identity (*efnb2a*, **m–p**; *notch1b*, **q–t**) and haemogenic endothelium *gata2b* (**u–x**) in uninjected (left column), Tfap2aMO (middle left column), Sox10MO (middle right column) or Sdc4MO (right column) embryos at 24 h.p.f. Scale bars = 100 μm. Percentages of embryos exhibiting the specified phenotypes relative to the appearance of expression in uninjected controls with total number (n) of embryos examined (**y**). See Supplementary Table 2.

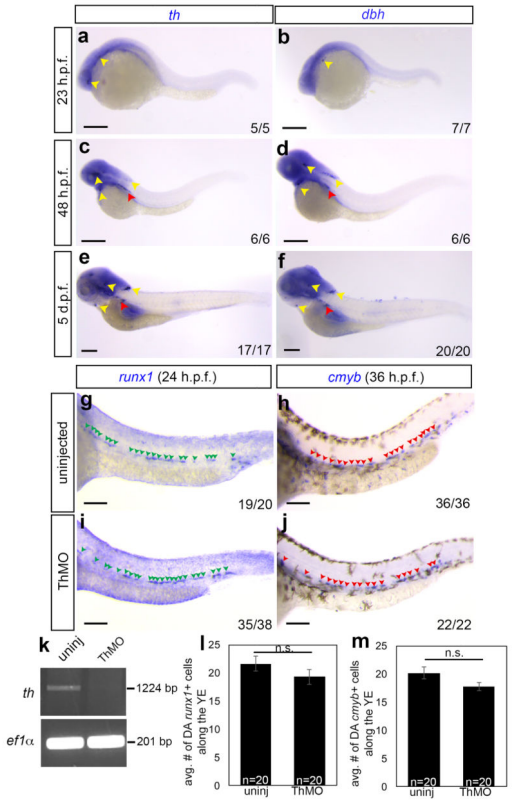

Figure 7. Catecholamine biosynthesis enzymes are not required for HSC specification

Lateral views (dorsal up, anterior left) of expression of the catecholamine biosynthesis enzymes *tyrosine hydroxylase* (*th;* **a, c, e**) and *dopamine-β-hydroxylase* (*dbh,* **b, d, f**) during (**a–b**) and after (**c–f**) HSC specification. Yellow arrowheads indicate expression in neurons of the head, red arrowheads indicate expression in the superior cervical ganglion. Numbers in the bottom right corner of panels indicate numbers of zebrafish embryos analysed for the indicated gene, versus the total number of zebrafish analysed. Zebrafish randomly selected from one clutch (**a–f**) or two clutches (**g–j**) are represented by the image. Scale bars = 200 μm. Expression of the HSC markers *runx1* (**g,i**) and *cmyb* (**h,j**) in uninjected (**g–h**) or Th morphant (**i–j**) embryos, at the indicated developmental stages green and red arrowheads indicate *runx1*$^{+}$ and *cmyb*$^{+}$ cells respectively in two separate experiments. Scale bars = 100 μm. RT-PCR showing a reduction in the amount of *th* mRNA in Th morphant compared to uninjected embryos. Average number of DA *runx1* (**l**) and *cmyb* (**m**) expressing cells in uninjected and Th morphants, n = 20 randomly selected zebrafish embryos, error bars indicate the standard error of the mean, n.s. = result not significant, p = 1.000 (**l**) and p = 0.0689 (**m**) by student's T-test. See Supplementary Table 3. Number of embryos displaying the depicted expression is indicated.